XLVI CILAMCE
VITÓRIA - ES - BRAZIL - 2025
XLVI IBERO-LATIN AMERICAN CONGRESS ON COMPUTATIONAL METHODS IN ENGENEERING

Extended-Regularized Lattice Boltzmann Method

Luís Orlando Emerich dos Santos[1], Diogo Nardelli Siebert[1], Ricardo Leite Martins Bazarin[1]

[1]*Dept. of Mobility Engineering, Federal University of Santa Catarina*
Rua Dona Francisca, 8300 – Bloco U Zona Industrial Norte, Joinville, 89.219-600, Santa Catarina, Brazil
luis.emerich@ufsc.br, diogo.siebert@ufsc.br, ricardo.bazarin@posgrad.ufsc.br

Abstract. The Lattice Boltzmann Method (LBM) is widely used for simulating fluid dynamics due to its flexibility and computational efficiency. However, the standard BGK collision model suffers from numerical instabilities, particularly in high Reynolds number flows. The Regularized Lattice Boltzmann Method (RLBM) improves stability by filtering out non-hydrodynamic moment. In this work we propose an extension of RLBM, which introduces a second relaxation time to further control high-order moments without compromising computational simplicity. Through numerical simulations, including the Taylor-Green vortex and a double shear layer test case, we demonstrate that our extended method significantly enhances numerical stability while maintaining accuracy. Our results suggest that tuning the relaxation time of non-hydrodynamic moments allows simulations at higher Reynolds numbers with improved robustness.

Keywords: Lattice Boltzmann Method, Regularization, Numerical Stability

1 Introduction

The Lattice Boltzmann Method (LBM) is a numerical approach widely employed for the simulation of fluid dynamics and related problems. Based on the kinetic theory of gases, the LBM can be seen as a discrete version of the Boltzmann transport equation with a lattice structure to represent the computational domain[1–4]. Since its inception in the 1980s and 1990s[5–7], the method has gained acceptance due to its flexibility in handling complex geometries and its inherently parallel nature, making it suitable for applications on modern computational architectures[8].

Due to its simplicity, the traditional BGK collision model (LBGK) is widely adopted[7]. It has, however, several limitations, including numerical instabilities and the introduction of non-physical artifacts, especially in simulations with high Reynolds numbers. In response to these challenges, the Regularized Lattice Boltzmann Method (RLBM) was developed[9–14]. This approach increases stability and accuracy by eliminating non-physical moments generated during the collision process, preserving only the relevant ones. The regularized method has proven effective in various applications, including turbulent flow simulations and multiphase systems, establishing itself as a robust alternative for scenarios demanding high numerical precision.

It is important to mention here that there are other alternatives for dealing with the limitations imposed by the BGK operator. One alternative is the use of multiple relaxation times (MRT model) [15–19]. Unlike the BGK model, which uses a single relaxation time for all moments, the MRT adopts multiple relaxation times, providing greater control over kinetic and hydrodynamic modes. In fact, both the RLBM and its extension proposed in this paper can be considered as simplifications of the MRT model. Another alternative is the so-called Entropic LBM which supplements the LBGK method with an H theorem[20–23]. The entropic approach has proven particularly effective in simulations of transient flows and under conditions with sharp gradients of velocity or density. Comparisons between the aforementioned methods, considering numerical stability and accuracy, can be found in the literature[12, 14, 24, 25].

The paper is structured as follows. Section 2 presents the LBGK and RLBM models. Then, in Section 3, an extension of the RLBM model – the Extended-Regularized Lattice Boltzmann Method (E-RLBM) – is proposed. Section 4 presents the simulations comparing the models. Section 5 concludes this work.

2 Lattice Boltzmann Method

As mentioned before, the LBM is a discretization of the Boltzmann transport equation. In this approach the fluid is described by a distribution function $f_i(\mathbf{x}, t)$ which represents the expected value of the number of particles at position $\mathbf{x}$, at time t with a velocity $\mathbf{c}_i$ ($i = 0, ..., q-1$). Space, time and velocities are discrete quantities, and the distribution function evolves in a collision-propagation scheme, according to the equation:

$$f_i(\mathbf{x} + \Delta t\, \mathbf{c}_i, t + \Delta t) = f_i(\mathbf{x}, t) + \Omega_i, \tag{1}$$

where Δt is the time step and Ω_i is the collision operator. The hydrodynamic variables (density and velocity) are moments of the distribution function:

$$\sum_i f_i(\mathbf{x}, t) = \rho(\mathbf{x}, t), \tag{2}$$

$$\sum_i f_i(\mathbf{x}, t)\mathbf{c}_i = \rho(\mathbf{x}, t)\mathbf{u}(\mathbf{x}, t). \tag{3}$$

Various collision operators can be used, the simplest being the BGK operator, which employs a single relaxation time (τ):

$$\Omega_i = \frac{f_i^{eq}(\mathbf{x}, t) - f_i(\mathbf{x}, t)}{\tau/\Delta t}, \tag{4}$$

where f_i^{eq} is the discrete equilibrium distribution (a Hermite polynomial expansion of the Maxwell-Boltzmann distribution), which is dependent on the discrete velocity space. It is possible to show that, depending on the chosen lattice (i.e., the discretization of the velocity space), as well as the order of the equilibrium distribution expansion, the system will evolve according to the Navier-Stokes equations[4][3] with the kinematic viscosity $\nu = c_s^2(\tau - \Delta t/2)$ and an ideal gas law pressure – the speed of sound c_s being related to the chosen lattice.

Equation (1) can be rewritten for LBGK as being

$$f_i^*(\mathbf{x}, t) = f_i^{eq}(\mathbf{x}, t) + \left(1 - \frac{\Delta t}{\tau}\right) f_i^{neq}(\mathbf{x}, t), \tag{5}$$

where $f_i^*(\mathbf{x}, t)$ is the post-collision distribution function, and $f_i^{neq} = f_i - f_i^{eq}$ is the non-equilibrium distribution.

In the (original) regularized LB scheme[10], the non-equilibrium distribution f_i^{neq} is replaced by the first-order approximation $f^{(1)}$, which is sufficient to represent the hydrodynamic moments,

$$f^{(1)} = \frac{\omega_i}{2c_s^4}(c_{i\alpha}c_{i\beta} - c_s^2\delta_{\alpha\beta})\Pi_{\alpha\beta}^{neq}, \tag{6}$$

$$\Pi_{\alpha\beta}^{neq} = \sum_i f_i^{neq} c_{i\alpha}c_{i\beta}; \tag{7}$$

where ω_i denote the lattice-dependent weight coefficients, $\delta_{\alpha\beta}$ is the Kronecker delta, and the Einstein summation convention is implied with the repeated indexes.

As a result of this procedure, the non-hydrodynamic moments are relaxed in one time step (they are filtered out), while the hydrodynamic moments are relaxed with τ.

3 Extended-Regularized Lattice Boltzmann Method

The regularization scheme can be extended by writing the collision process as

$$f_i^*(\mathbf{x},t) = f_i^{eq}(\mathbf{x},t) + \left(1 - \frac{\Delta t}{\tau}\right) f_i^{(1)}(\mathbf{x},t) + \left(1 - \frac{\Delta t}{\tau_{nh}}\right) f_i^{(>1)}(\mathbf{x},t), \tag{8}$$

where $f_i^{(>1)} = f_i - f_i^{eq} - f_i^{(1)}$ is related to the high-order terms in the f_i distribution and τ_{nh} is the relaxation time of the non-hydrodynamic moments.

Of course, if $\tau_{nh} = \Delta t$, we recover the regularized model, while $\tau_{nh} = \tau$ results in the BGK model. However, any value of τ_{nh} can be chosen, as it will not affect the hydrodynamic moments. In other words, we can choose values of τ_{nh} in order to increase the numerical stability of the model.

Before moving on to the simulations section, it is important to discuss another topic related to the numerical stability of the simulations: the equilibrium distributions f_i^{eq} – which are, as we mentioned before, Hermite polynomial expansions of the Maxwell-Boltzmann distribution. In simulations of isothermal problems, it is sufficient to consider terms up to second order in the expansion. The lattices used (that is, the discretization of the velocity space) are related to the order considered in the expansion. The most commonly used lattices – the D2Q9 and D3Q19 lattices – allow an adequate representation of a second-order expansion and, therefore, are suitable for simulating isothermal hydrodynamic problems. Including higher-order terms in the equilibrium distribution, while maintaining the discretization of the velocity space, can considerably increase numerical stability, although it can reduce the accuracy of the simulations.

To understand why this happens, we must briefly analyze the causes of numerical instabilities. The LBM dynamics can be divided into two steps: collision and propagation. The propagation step simply translates the distributions from one position to another and, therefore, in itself, cannot cause a simulation to diverge. Therefore, the collision step is responsible for numerical instabilities. Considering that *diverge* means that the distributions at a given point assume absolute values greater than what can be numerically represented, and that the collision process conserves mass – that is, a finite mass before the collision remains the same finite mass after the collision – the only way for a simulation to diverge is if one or more distributions assume negative values. In this case, one distribution tends to $+\infty$ and the other to $-\infty$, but the total mass at the point remains the same.

Consequently, finding what makes a simulation diverge is finding what makes a distribution take on negative values (this is a necessary condition, not a sufficient one). There are two, not mutually exclusive, ways in which this can happen: (1) – when the velocities are high, which causes f_i^{eq} to become negative; (2) – when the relaxation time τ is shorter than the time step Δt, which makes $(1 - \Delta t/\tau) f_i^{eq} < 0$, and can cause a distribution to become negative.

Procedures like the regularization addresses the second cause, while the inclusion of high order therms in the equilibrium distribution addresses the first one.

4 Simulations

In this section, we present simulation results comparing the stability and accuracy of the collision operators presented in the previous section. The simulations were carried out using a D2Q9 lattice.

4.1 Stability Maps

The two-dimensional (2D) decaying Taylor–Green vortex [26] was chosen as a first test case to study the stability of the models. The initial conditions for the velocity field are as follows

$$u_x = U_0 \sin(kx)\cos(ky), \tag{9}$$
$$u_y = -U_0 \cos(kx)\sin(ky), \tag{10}$$

where $k = 2\pi/L$ is the wave number, L being the length computational domain in both directions, and periodic boundary conditions were applied. With regard to the initial pressure field, this was obtained by solving Poisson's equation through an iterative process, as described in [27]

Since the stability of the simulations depends on both the viscosity, ν, and the initial velocity, U_0, *stability maps* were constructed, in which the initial velocity (in fact, the Mach number, $Ma = U_0/c_s$) is represented on the x-axis and the viscosity (in fact, $\log(\nu)$) is represented on the y-axis. We consider the simulation to have diverged if the total kinetic energy becomes greater than the initial total kinetic energy, in which case we represent the point

as black. As expected, the BGK model (Fig. 1(a)) proved to be more unstable. The RLBM (Fig. 1(b)) presents a considerably larger region of stability. However, the with E-RLBM we were able to expand the stability region (Fig. 1(c)). As mentioned in the previous section, the inclusion of terms up to 4th order increases the stability region (see Fig. 1(d)), especially for high velocities. In the simulations presented in Fig. 1(c) and Fig. 1(d), we used a non-hydrodynamic relaxation time $\tau_{nh} = 0.65$.

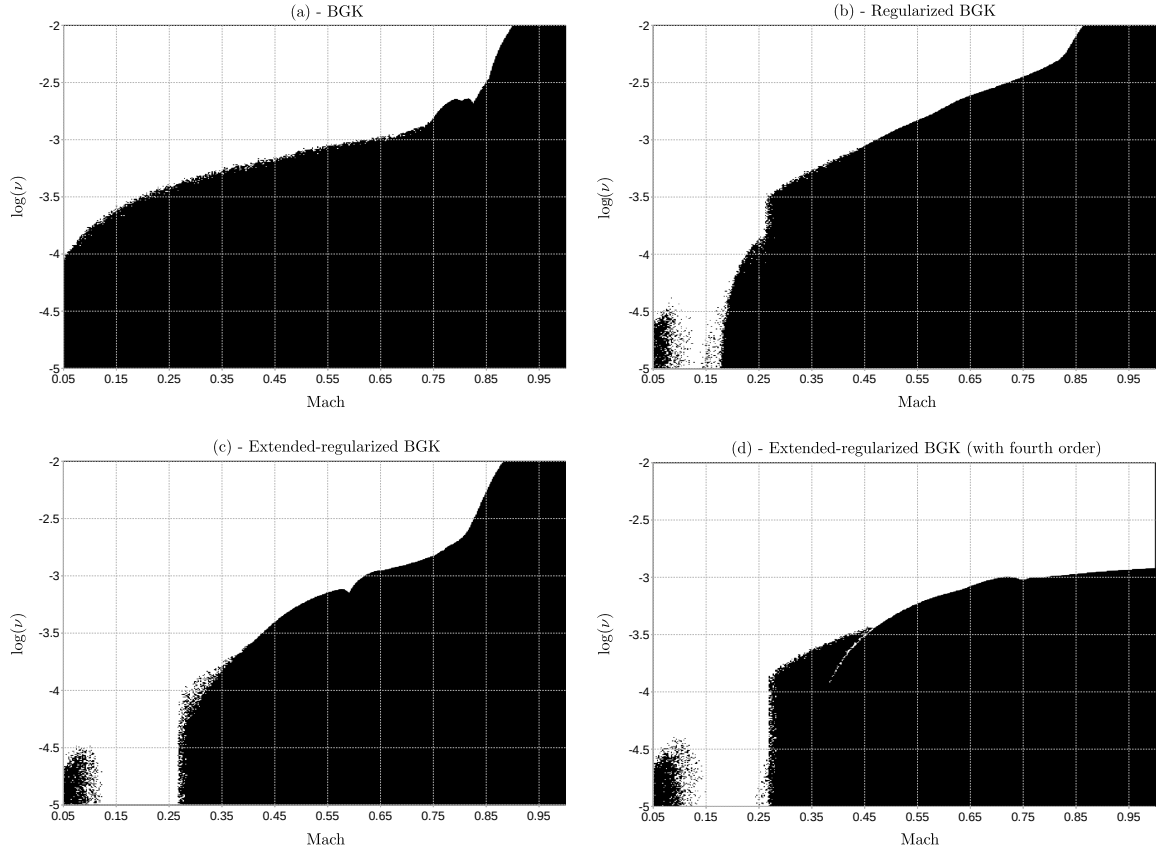


Figure 1. Stability maps of collision models constructed from Taylor-Green vortex simulations. The black regions represent the positions (in terms of viscosity and initial velocity) where the simulations diverge.

4.2 Accuracy

Stability does not imply accuracy or convergence to a meaningful result. To study this second point, we simulate two classic test cases: Taylor-Green vortex, for low Reynolds numbers ($Re = 50$); and Double Shear Layer[28] for higher Reynolds numbers ($Re = 20000$ and $Re = 80000$). In both cases the Reynolds number is defined as $Re = U_0 L/\nu$ and the characteristic time as $T = L/U_0$.

For low Reynolds numbers the incompressible Taylor-Green vortex – already seen in subsection 4.1 – has the following analytic solutions to the incompressible Navier–Stokes equation in two dimensions:

$$u_x(x, y, t) = U_0 \sin(kx) \cos(ky) e^{-2\nu k^2 t}, \tag{11}$$

$$u_y(x, y, t) = -U_0 \cos(kx) \sin(ky) e^{-2\nu k^2 t}. \tag{12}$$

Initially, we simulated five cases, with L varying from 32 to 512, $Re = 50$ and $U_0 = 1/16$. Deviation from the analytical solution was calculated with a L_2 error norm:

$$L_2 = \sqrt{\frac{\sum (u_S - u_R)^2}{\sum u_R^2}} \tag{13}$$

where $u_R = \sqrt{\mathbf{u}_R \cdot \mathbf{u}_R}$ is the reference (analytical) solution for the velocity field, and u_S is the simulated result.

A comparison of the simulated results with the analytical solution is shown in the Fig. 2. A similar behavior can be seen in which all the models converge on the same result, with an L_2 error of the order of 10^{-4}.

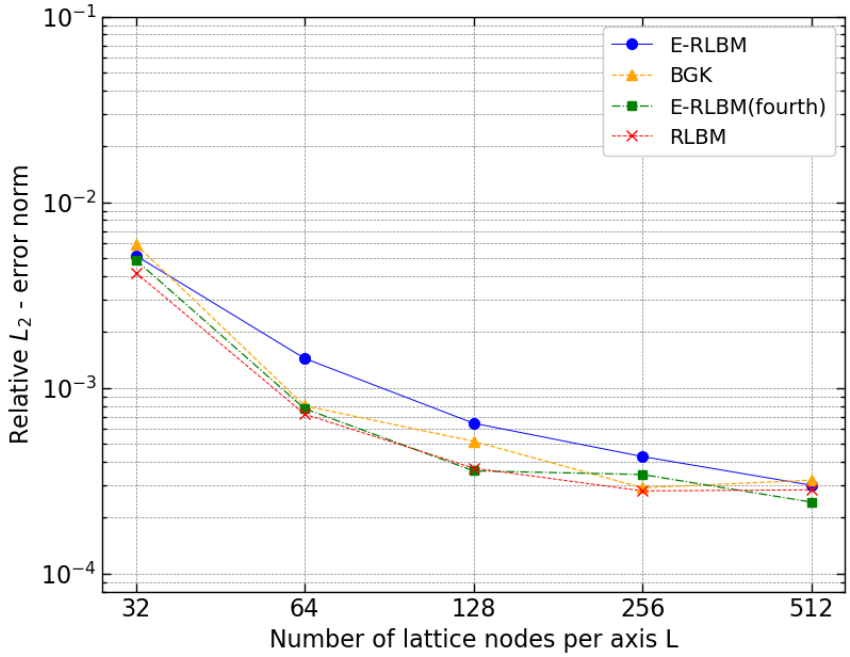


Figure 2. Error in relation to the analytical solution for the case of Taylor-Green vortex. Reynolds number is equal to $Re = 50$, initial velocity is $U_0 = 1/16$.

The second test case simulated to evaluate the accuracy of the proposed model was the double shear layer flow. Similar to the Taylor-Green vortex, this simulation is also periodic. The flow starts with two antiparallel shear layers and a small velocity disturbance, perpendicular to the shear flow directions. This causes the antiparallel shear layers to curl and leads to spiral-shaped vorticity patterns. The initial velocity field, which includes the shear layers and the disturbance, is given by:

$$u_x = \begin{cases} U_0 \tanh\left[\lambda\left(\frac{y}{L} - \frac{1}{4}\right)\right], & y \leq \frac{L}{2}, \\ U_0 \tanh\left[\lambda\left(\frac{3}{4} - \frac{y}{L}\right)\right], & y > \frac{L}{2}, \end{cases} \tag{14}$$

$$u_y = \epsilon U_0 \sin\left[2\pi\left(\frac{x}{L} + \frac{1}{4}\right)\right], \tag{15}$$

where U_0 defines the amplitude of the initial velocities. The computational domain has length L in both directions and the parameters λ and ϵ control, respectively, the width of the shear layer and the initial velocity perturbation. In all simulations, we used $\lambda = 80$ and $\epsilon = 0.05$.

To determine the convergence of the models studied, we first simulated a reference case, using RLBM, with $L = 2048$ and $U_0 = 1/32$. Simulations were carried out with Reynolds number equal to 80000 (Fig. 3), with L varying from 64 to 1024, and initial velocity $U_0 = 1/32$ in all cases. The results show that there are no significant difference between the RLBM and E-RLBM for the non-hydrodynamic relaxation times chosen (which imply greater stability). The inclusion of fourth-order terms in the equilibrium distribution, however, prevents the simulation from converging to the reference solution.

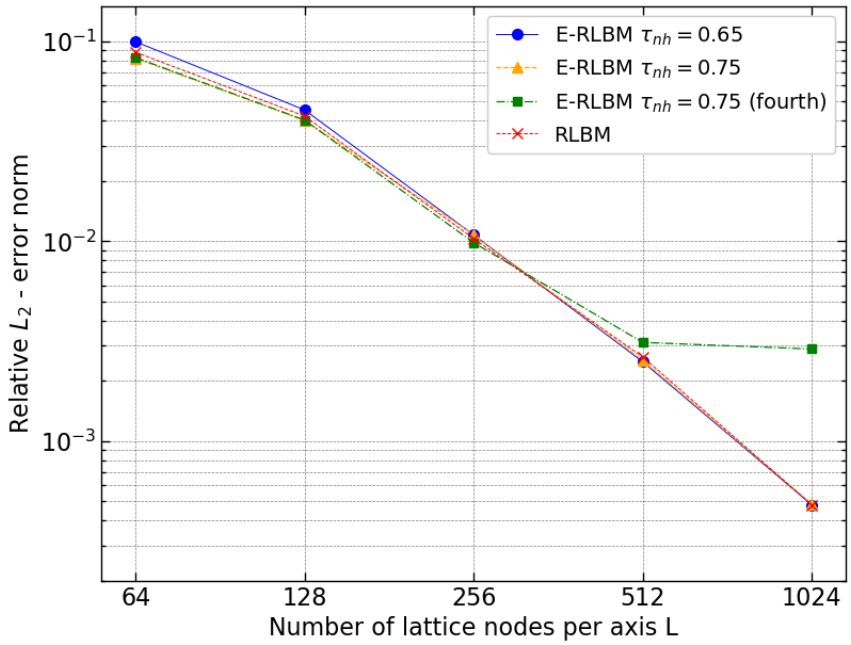


Figure 3. Convergence of the numerical error for reference solution (RLBM, using $L = 2048$); $Re = 80000$ and $U_0 = 1/32$. The errors are measured at $t = T$.

5 Conclusions

In this work, we proposed an extension of the regularized LBM model by incorporating a second relaxation time acting on the high-order (non-hydrodynamic) moments. We demonstrated that an appropriate choice of this second relaxation time enhances stability, allowing the simulation of higher Reynolds numbers without compromising the model's accuracy. Furthermore, we showed that the inclusion of fourth-order terms in the equilibrium distribution, while increasing stability – particularly for higher Mach numbers – reduces the model's accuracy.

All simulations conducted in this study were isothermal. It is expected that the introduction of the second relaxation time may affect non-isothermal simulations, possibly altering thermal conductivity. This aspect should be the subject of future investigations.

Acknowledgements. We gratefully acknowledge the support and sponsorship by Equinor Brazil (Project ANP 23270-2). We also acknowledge the support of ANP (Brazil National Oil, Natural Gas and Biofuels Agency) through the R&D levy.

Authorship statement. The authors hereby confirm that they are the sole liable persons responsible for the authorship of this work, and that all material that has been herein included as part of the present paper is the property (and authorship) of the authors.

References

[1] T. Abe. Derivation of the Lattice Boltzmann Method by Means of the Discrete Ordinate Method for the Boltzmann Equation. *Journal of Computational Physics*, vol. 131, pp. 241–246, 1997.
[2] L.-S. Luo. Theory of the lattice boltzmann method: From the boltzmann equation to the lattice boltzmann equation. *Physical Review E*, vol. 56, n. 6, pp. 6811–6817, 1997.
[3] P. Philippi, L. H. Jr, L. D. Santos, and R. Surmas. From the continuous to the lattice boltzmann equation: The discretization problem and thermal models. *Physical Review E*, vol. 73, n. 5, pp. 056702, 2006.
[4] X. Shan, X. F. Yuan, and H. Chen. Kinetic theory representation of hydrodynamics: A way beyond the Navier-Stokes equation. *Journal of Fluid Mechanics*, vol. 550, pp. 413–441, 2006.
[5] G. R. McNamara and G. Zanetti. Use of the Boltzmann equation to simulate lattice-gas automata. *Physical review letters*, vol. 61, n. 20, pp. 2332, 1988.

[6] F. J. Higuera and J. Jimenez. Boltzmann approach to lattice gas simulations. *Europhys. Lett.*, vol. 9, pp. 663, 1989.
[7] Y. H. Qian, D. d'Humières, and P. Lallemand. Lattice BGK models for Navier-Stokes equation. *EPL (Europhysics Letters)*, vol. 17, n. 6, pp. 479, 1992.
[8] T. Krüger, H. Kusumaatmaja, A. Kuzmin, O. Shardt, G. Silva, and E. M. Viggen. *The Lattice Boltzmann Method: Principles and Practice*. Springer International Publishing, 2017.
[9] A. J. C. Ladd and R. Verberg. Lattice-boltzmann simulations of particle-fluid suspensions. *Journal of Statistical Physics*, vol. 104, pp. 1191–1251, 2001.
[10] J. Latt and B. Chopard. Lattice boltzmann method with regularized pre-collision distribution functions. *Mathematics and Computers in Simulation*, vol. 72, n. 2–6, pp. 165–168, 2006.
[11] O. Malaspinas. Increasing stability and accuracy of the lattice boltzmann scheme: recursivity and regularization, 2015.
[12] C. Coreixas, G. Wissocq, G. Puigt, J.-F. Boussuge, and P. Sagaut. Recursive regularization step for high-order lattice boltzmann methods. *Physical Review E*, vol. 96, n. 3, 2017.
[13] K. K. Mattila, P. C. Philippi, and L. A. Hegele. High-order regularization in lattice-boltzmann equations. *Physics of Fluids*, vol. 29, n. 4, 2017.
[14] A. Jonnalagadda, A. Sharma, and A. Agrawal. Onsager-regularized lattice boltzmann method: A nonequilibrium thermodynamics-based regularized lattice boltzmann method. *Physical Review E*, vol. 104, n. 1, 2021.
[15] P. Lallemand and L.-S. Luo. Theory of the lattice boltzmann method: Dispersion, dissipation, isotropy, galilean invariance, and stability. *Physical Review E*, vol. 61, n. 6, pp. 6546–6562, 2000.
[16] D. d'Humières. Multiple–relaxation–time lattice boltzmann models in three dimensions. *Philosophical Transactions of the Royal Society of London. Series A: Mathematical, Physical and Engineering Sciences*, vol. 360, n. 1792, pp. 437–451, 2002.
[17] D. d'Humières and I. Ginzburg. Viscosity independent numerical errors for lattice boltzmann models: From recurrence equations to "magic" collision numbers. *Computers & Mathematics with Applications*, vol. 58, n. 5, pp. 823–840, 2009.
[18] Y. Ning, K. N. Premnath, and D. V. Patil. Numerical study of the properties of the central moment lattice boltzmann method. *International Journal for Numerical Methods in Fluids*, vol. 82, n. 2, pp. 59–90, 2015.
[19] M. Geier, M. Schönherr, A. Pasquali, and M. Krafczyk. The cumulant lattice boltzmann equation in three dimensions: Theory and validation. *Computers & Mathematics with Applications*, vol. 70, n. 4, pp. 507–547, 2015.
[20] I. V. Karlin, A. Ferrante, and H. C. Öttinger. Perfect entropy functions of the lattice boltzmann method. *Europhysics Letters (EPL)*, vol. 47, n. 2, pp. 182–188, 1999.
[21] S. Ansumali and I. V. Karlin. Stabilization of the lattice boltzmann method by the h theorem: a numerical test. *Physical Review E*, vol. 62, n. 6, pp. 7999–8003, 2000.
[22] I. V. Karlin, F. Bösch, and S. S. Chikatamarla. Gibbs' principle for the lattice-kinetic theory of fluid dynamics. *Physical Review E*, vol. 90, n. 3, 2014.
[23] M. Atif, P. K. Kolluru, C. Thantanapally, and S. Ansumali. Essentially entropic lattice boltzmann model. *Physical Review Letters*, vol. 119, n. 24, 2017.
[24] K. K. Mattila, L. A. Hegele, and P. C. Philippi. Investigation of an entropic stabilizer for the lattice-boltzmann method. *Physical Review E*, vol. 91, n. 6, 2015.
[25] C. Coreixas, B. Chopard, and J. Latt. Comprehensive comparison of collision models in the lattice boltzmann framework: Theoretical investigations. *Physical Review E*, vol. 100, n. 3, 2019.
[26] G. I. Taylor and A. E. Green. Mechanism of the production of small eddies from large ones. *Proceedings of the Royal Society of London. Series A, Mathematical and Physical Sciences*, vol. 158, pp. 499–521, 1937.
[27] R. Mei, L.-S. Luo, P. Lallemand, and D. d'Humières. Consistent initial conditions for lattice boltzmann simulations. *Computers & Fluids*, vol. 35, n. 8–9, pp. 855–862, 2006.
[28] M. L. Minion and D. L. Brown. Performance of under-resolved two-dimensional incompressible flow simulations, ii. *Journal of Computational Physics*, vol. 138, n. 2, pp. 734–765, 1997.